

Exact generation of quantum states by the dynamics of spin chains

Morteza Moradi, Vahid Karimipour

Department of Physics, Sharif University of Technology, P.O. Box 11155-9161, Tehran, Iran.

Abstract

We design a quasi-one-dimensional spin chain with engineered coupling strengths such that the natural dynamics of the spin chain evolves a single excitation localized at the left-hand site to any specified single particle state on the whole chain. Our treatment is an exact solution to a problem which has already been addressed in approximate ways. As two important examples, we study the W states and Gaussian states with arbitrary width.

PACS numbers: 89.70.+c, 03.65

1 Introduction

Quantum spin chains, apart from being an indispensable tool for understanding a large variety of phenomena in condensed matter physics, have also been a large laboratory for the investigation of exactly solvable models in many-body quantum systems. One of the main goals in these disciplines has been to find specific quantum spin chains for which the ground state and correlation functions can be found in closed form. With the upsurge of quantum computation and information theory, it is now almost a decade that the dynamics of spin chains has attracted attention in connection with quantum information processing tasks [1–9, 12, 14–19]. Starting with [1], spin chains turned out to be excellent carriers of quantum states in short distances either with very high or with perfect fidelity [3–9]. Since then the plethora of quantum information tasks for quantum spin chains has considerably expanded, including entanglement distribution [10–12], measurement-based quantum computation [13–15], perfect routings [16–18] and quite recently state generation [19] which is the subject of the present paper. The importance of this problem, that is the capability of initializing a quantum register to any given state cannot be overemphasized. Such a problem will have many applications, i.e. in quantum simulations among other domains. Here the goal is to design a specific Hamiltonian which can evolve a single excitation which is completely localized on one site to a given desired state which is distributed over all spins.

More precisely, given a state

$$|\psi\rangle = \sum_{k=1}^N \psi_k |k\rangle, \quad (1)$$

the idea is to design a Hamiltonian such that after a time t_0 , we have

$$|\psi\rangle = e^{-iHt_0} |1\rangle.$$

Here $|k\rangle$ means the state $|0, \dots, 0, 1, 0 \dots 0\rangle$ where only the spin on site k is excited. The states $\{|k\rangle, k = 1 \dots N\}$ span the one-excitation sector of the Hilbert space. Naturally here we have in mind those Hamiltonians which conserve the number of excitations and hence commute with the total spin operator, i.e. $[H, S_z] = 0$. A prototype of these Hamiltonians is the XY Hamiltonian given by

$$H = \sum_{n=1}^N \frac{B_n}{2} (1 - Z_n) + \sum_{n=1}^{N-1} J_n (X_n X_{n+1} + Y_n Y_{n+1}),$$

where X_n, Y_n , and Z_n are the Pauli matrices acting on site n . Recently this problem was posed and investigated in [19], where it was shown that provided that no two consecutive amplitudes of $|\psi\rangle$ are zero, the local magnetic fields B_n and the local couplings J_n can be engineered in such a way that $|\psi\rangle$ can be generated with arbitrary precision. However, the actual values of couplings B_n and J_n had to be found numerically and by iteratively tuning the Hamiltonian. As admitted in [19] the disadvantage of this numerical method was that the time t_0 scaled as N^2 , making the process rather slow. To remedy this, the author of [19] proposed an alternative analytical method which could produce only a very limited number of states. One could then hope that by using various perturbative techniques one could deform these states so that the given state can be approximated.

Our goal in this paper is to solve the problem of state generation analytically for all one-particle states in an exact way. To this aim, we utilize a quasi-one-dimensional chain shown in Fig.1(a). The crucial point for this kind of geometry is that the chain decomposes into a direct sum of virtual chains of two spins for which the evolution of an excitation is extremely simple. It is this decomposition and the subsequent simplicity of the dynamics which allows an exact determination of the couplings for all kinds of states. While in [19], this problem is connected to an inverse eigenvalue problem which is solved iteratively, here we solve the problem by exactly and simultaneously following the evolution of the particles (more precisely the probability amplitudes of a single particle) on all the small chains. This leads to a set of coupled non-linear equations for the couplings which we solve in closed form. We should remind that there are other quasi-one-dimensional chains [16] which have a simple apparent geometry than the one shown in Fig.1(a). However, they decompose into virtual chains of length two and three and it is not easy to simultaneously follow the dynamics of the particles as described above and solve the subsequent non-linear equations.

In summary for any state of the form (1), we exactly determine the coupling constants J_n and the times t_n for applying the single qubit Z_n gates. As examples, we consider the generation of W states and Gaussian states of various width on chains of different lengths. The results for these examples are shown in figures 3 and 5.

Remark: We should emphasize that compared to the method of [19], which uses a time-independent Hamiltonian and generates a limited class of single-particle states, the price that we pay for this exact generation of all single-particle states, is that we need to apply local single qubit Z gates at specific times. This substitutes the tuning of local albeit static magnetic fields on all sites proposed in [19]. The extent to which the timing of these pulses is crucial for the success of the scheme is discussed in section (5).

The structure of the paper is as follows: in section 2 we simply analyze the structure of the quasi-one-dimensional chain and its equivalence to the virtual 2-chains and examine the dynamics of the chain. In section 3 we determine the coupling constants and the times for applying the Z -pulses. Section 4 is devoted to examples where we study two important classes of examples, namely the W -states and the Gaussian states. We end the paper with an outlook.

2 The spin network structure

We introduce the spin network shown in Fig.1(a) where each link entails a Hamiltonian $h := \frac{1}{2}(X \otimes X + Y \otimes Y)$ with strength J written on the link. As is seen in each block all the interaction of horizontal and oblique links are equal modulo the signs. It is known that in architectures based on Josephson Junction superconducting qubits, which are modeled by XX Hamiltonians, it is possible to implement couplings with negative signs [20]. The main point is that in the one-particle sector the Hamiltonian h is nothing but a simple hopping term. In fact, it is well known and easily verified that

$$h_{i,j} = \frac{1}{2}(X_i X_j + Y_i Y_j) = |i\rangle\langle j| + |j\rangle\langle i|. \quad (2)$$

Therefore $h|0,0\rangle = h|1,1\rangle = 0$, $h|0,1\rangle = |1,0\rangle$ and $h|1,0\rangle = |0,1\rangle$.

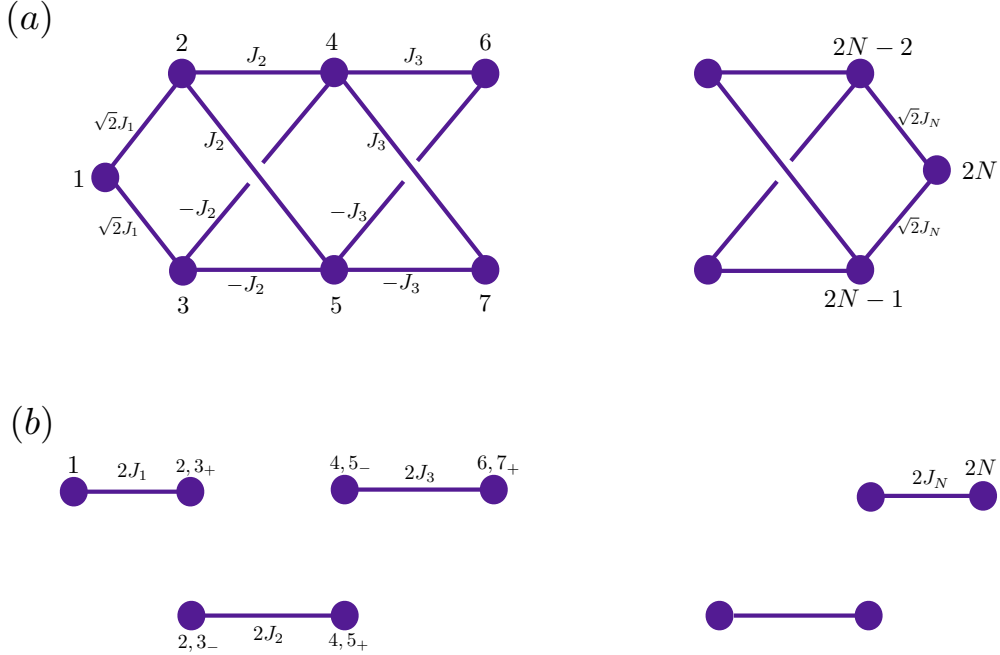


Figure 1: (a) A spin network containing two 1-D chains with regular interaction between them. The vertices represent qubits, and the edges used to show XX coupling between qubits of strength J_k . (b) N virtual spin chains of length 2 equivalent to the spin network in (a). The coupling strengths are shown on the edges. In our examples, we use the lower part of the network, the sites with odd index, only as ancillary qubits. That is the amplitude on all these sites are zero and the state is supported only on the above leg of the chain, i.e. on the even-numbered spins.

As the XX Hamiltonian commutes with Z_n :

$$[H, \sum_{i=1}^N Z_i] = 0,$$

if we start from a single excitation in site 1 or any other site, the dynamics will be confined in the

one-particle sector. One can now consider an arbitrary block like the one containing the spins 2, 3, 4 and 5. The part of Hamiltonian pertaining to these spins can be rewritten as

$$\begin{aligned} H_1 &= J_2(|2\rangle\langle 4| + |2\rangle\langle 5| - |3\rangle\langle 4| - |3\rangle\langle 5|) + h.c. \\ &= J_2(|2\rangle - |3\rangle)(\langle 4| + \langle 5|) + h.c. = 2J_2(|2, 3_-\rangle\langle 4, 5_+|) + h.c., \end{aligned} \quad (3)$$

where $\forall i, j \in \{1, 2, \dots, 2N\} : |i, j_\pm\rangle := \frac{1}{\sqrt{2}}(|i\rangle \pm |j\rangle)$. The same analysis applies to the next block whose Hamiltonian is rewritten as

$$\begin{aligned} H_2 &= J_3(|4\rangle\langle 6| + |4\rangle\langle 7| - |5\rangle\langle 6| - |5\rangle\langle 7|) + h.c. \\ &= J_3(|4\rangle - |5\rangle)(\langle 6| + \langle 7|) + h.c. = 2J_3(|4, 5_-\rangle\langle 6, 7_+|) + h.c.. \end{aligned} \quad (4)$$

Noting that all the states written in the right-hand side of (3) and (4) are orthogonal to each other, it turns out that the chain decomposes into a collection of spin chains of length 2 shown in Fig.1(b). With the definitions $|0, 1_-\rangle := |1\rangle, |2N, 2N + 1_+\rangle := |2N\rangle$, the final Hamiltonian can be written as a collection of independent 2-spin chains, as in Fig.1(b):

$$H = \sum_{n=1}^N 2J_n |2n - 2, 2n - 1_-\rangle\langle 2n, 2n + 1_+| + h.c. \quad (5)$$

3 Dynamics in the spin network

If we were to use this chain for perfect state transfer, our task would be more straightforward. We only needed to move a single excitation from site 1 to site 23_+ and then apply a Z-pulse to site 3 to move the excitation from the site 23_+ to 23_- and put it on the beginning of the next chain which automatically goes over to the end of this site after a certain time and then repeat the process until the excitation reaches the other end of the total chain. However, in generating states we want to distribute the excitation with prescribed probabilities all over the chain and hence also all over the virtual chains. This is a much harder task than state transfer in which when the excitation leaves a virtual 2-spin chain, we do not need to take it into account anymore. Here as times passes we have to know how all the excitations in all the 2-chains (more precisely the probabilities of a single excitation in all the 2-chains) evolve in time. This is where the dynamics of a 2-spin chain, compared with a 3-spin chain plays a crucial role. Denoting the two sites of a 2-chain simply by 1 and 2, we have

$$H = J\mathbf{X}_1 \cdot \mathbf{X}_2 \equiv \frac{J}{2}(X_1 \otimes X_2 + Y_1 \otimes Y_2) = J(|1\rangle\langle 2| + |2\rangle\langle 1|) = \begin{bmatrix} 0 & J \\ J & 0 \end{bmatrix},$$

and hence

$$e^{-iHt}|1\rangle = \cos(Jt)|1\rangle - i \sin(Jt)|2\rangle. \quad (6)$$

Let us start from the state $|1\rangle$. The dynamics of the chain evolves this state after time t_1 within the leftmost chain:

$$e^{-iHt_1}|1\rangle = \cos(2J_1 t_1)|1\rangle - i \sin(2J_1 t_1)|2, 3_+\rangle$$

Applying the Z_3 gate at time t_1 turns this into

$$Z_3 e^{-iHt_1}|1\rangle = \cos(2J_1 t_1)|1\rangle - i \sin(2J_1 t_1)|2, 3_-\rangle.$$

The excitation is now on both site 1 of the first 2-chain and site 23_- of the second 2-chain with the indicated amplitudes. After time t_2 both amplitudes evolve and after the pulse Z_5 we have

$$\begin{aligned} Z_5 e^{-iHt_2} Z_3 e^{-iHt_1} |1\rangle &= \cos(2J_1 t_1) \left[\cos(2J_1 t_2) |1\rangle - i \sin(2J_1 t_2) |2, 3_+\rangle \right] \\ &\quad - i \sin(2J_1 t_1) \left[\cos(2J_2 t_2) |2, 3_-\rangle - i \sin(2J_2 t_2) |4, 5_-\rangle \right]. \end{aligned}$$

We can continue in this manner to find the state of the chain under the following dynamics

$$|\psi\rangle = e^{-iHt} |1\rangle := e^{-iHt_N} Z_{2N-1} e^{-iHt_{N-1}} \dots Z_5 e^{-iHt_2} Z_3 e^{-iHt_1} |1\rangle. \quad (7)$$

To find the amplitudes in a simpler way, a descriptive way is very effective: After the pulse Z_3 which is applied at t_1 , a fraction $-i \sin(2J_1 t_1)$ is at the beginning of the second chain, namely on 23_- . After the pulse Z_5 which is applied at t_2 , a fraction $-i \sin(2J_2 t_2)$ of this amplitude moves to the beginning of the third chain, namely on site $4, 5_-$. Continuing in this way, after the pulse Z_{2k-1} which is applied at time t_{k-1} , the excitation has reached the site $(2k-2, 2k-1)_-$ with an amplitude

$$(-i \sin(2J_1 t_1)) (-i \sin(2J_2 t_2)) \dots (-i \sin(2J_{k-1} t_{k-1})) =: (-i)^{k-1} A_{k-1}.$$

With the next pulse at site Z_{2k+1} a fraction $-i \sin(2J_k t_k)$ of this amplitude leaves this chain and a fraction $\cos(2J_k t_k)$ remains in the chain. It is now important that all the other applied pulses on sites $2k+3, 2k+5, \dots$ do not affect this amplitude which hereafter changes only by the internal dynamics of the short chain $[(2k-2, 2k-1)_-, (2k, 2k+1)_+]$. Thus the explicit form of the wave function is given by:

$$\begin{aligned} |\psi\rangle &= \sum_{k=1}^N (-i)^{k-1} A_{k-1} \cos(2J_k(\tau_k - \tau_{k+1})) \cos(2J_k \tau_{k+1}) |2k-2, 2k-1_-\rangle \\ &\quad + \sum_{k=1}^N (-i)^k A_{k-1} \cos(2J_k(\tau_k - \tau_{k+1})) \sin(2J_k \tau_{k+1}) |2k, 2k+1_+\rangle. \end{aligned} \quad (8)$$

where

$$\tau_k := \sum_{i=k}^N t_i \quad ; \quad \tau_{N+1} := t_N, \quad (9)$$

and

$$A_k := \prod_{i=1}^k \sin(2J_i t_i) \quad ; \quad A_0 := 1. \quad (10)$$

Now, we have to calculate the times and coupling strengths such that our intended arbitrary state (1) will be generated. For the time being, we focus on the absolute squares of all the coefficients in (1) as positive. Once the state with the required probabilities is generated on the chain, we can apply phase gates $e^{iZ_k \phi_k}$ to tune also the local phases.

3.1 Calculating the times and coupling strengths

Consider now a state $|\psi\rangle$ with some given amplitudes on the virtual chains. In this section, we first calculate the times t_k and coupling strengths J_k to create this state. We will then relate both these amplitudes and the corresponding times and coupling strengths to the actual quasi-one-dimensional chain in Fig.1(a).

3.1.1 Given probability amplitudes in the virtual spin chains

We first consider the virtual chain. The probabilities on the sites of this chain are denoted by $\{q_k\}$ and those on the actual chain are denoted by $\{p_k\}$, figure (2). Suppose that q_{2k+1} and q_{2k} are respectively the probabilities that $|2k, 2k+1_- \rangle$ and $|2k, 2k+1_+ \rangle$ are excited. Thus from the equation (8):

$$\begin{aligned} q_{2k-1} &= [A_{k-1} \cos(2J_k(\tau_k - \tau_{k+1})) \cos(2J_k \tau_{k+1})]^2 \\ q_{2k} &= [A_{k-1} \cos(2J_k(\tau_k - \tau_{k+1})) \sin(2J_k \tau_{k+1})]^2, \end{aligned} \quad (11)$$

where A_k is given in (10). From this set of coupled nonlinear equations, we should determine all the times t_k and all the coupling constants J_k . First, we divide the second equation of (11) by the first to obtain $\tan^2(2J_k \tau_{k+1}) = \frac{q_{2k}}{q_{2k-1}}$, or

$$\cos^2(2J_k \tau_{k+1}) = \frac{q_{2k-1}}{q_{2k-1} + q_{2k}}. \quad (12)$$

Remark: In case that two consecutive probabilities q_{2k-1} and q_{2k} are zero, we only need to set $2J_k(\tau_k - \tau_{k+1}) = \frac{\pi}{2} + m\pi$ and choose the parameter $2J_k \tau_{k+1} = N\pi$ see the explanation before equation (17). Therefore in contrast to the method in [19], such states can also be generated by our method.

Second, the sum of the two equations in (11) leads to

$$q_{2k-1} + q_{2k} = A_{k-1}^2 \cos^2(2J_k(\tau_k - \tau_{k+1})). \quad (13)$$

Using (13) we find,

$$\begin{aligned} A_k^2 &= \prod_{i=1}^k \sin^2(2J_i(\tau_i - \tau_{i+1})) = A_{k-1}^2 \sin^2(2J_k(\tau_k - \tau_{k+1})) \\ &= A_{k-1}^2 (1 - \cos^2(2J_k(\tau_k - \tau_{k+1}))) = A_{k-1}^2 - (q_{2k-1} + q_{2k}). \end{aligned}$$

By repeating this argument and using

$$A_1^2 = 1 - q_1 - q_2$$

we find

$$A_k^2 = 1 - \sum_{i=1}^{2k} q_i = \sum_{i=2k+1}^{2N} q_i.$$

This already leads to a very simple result: despite its appearance as indicated in (10), A_k is a time-independent quantity which is solely determined by the probabilities. From (13), we obtain

$$\cos^2(2J_k(\tau_k - \tau_{k+1})) = \frac{q_{2k-1} + q_{2k}}{A_{k-1}^2}. \quad (14)$$

Equations (12) and (14), give the sequence of ratios $\frac{\tau_{k+1}}{\tau_k}$ which finally leads to the determination of all τ_k 's in terms of τ_1 and then to the determination of all the coupling constants J_k . There are some important details, due to the multiple solutions of these equations, which we describe below.

Equation (11) gives

$$2J_k \tau_{k+1} = n_k \pi + \cos^{-1} \sqrt{\frac{q_{2k-1}}{q_{2k-1} + q_{2k}}}, \quad n_k \in \mathbb{Z} \quad k = 1, \dots, N, \quad (15)$$

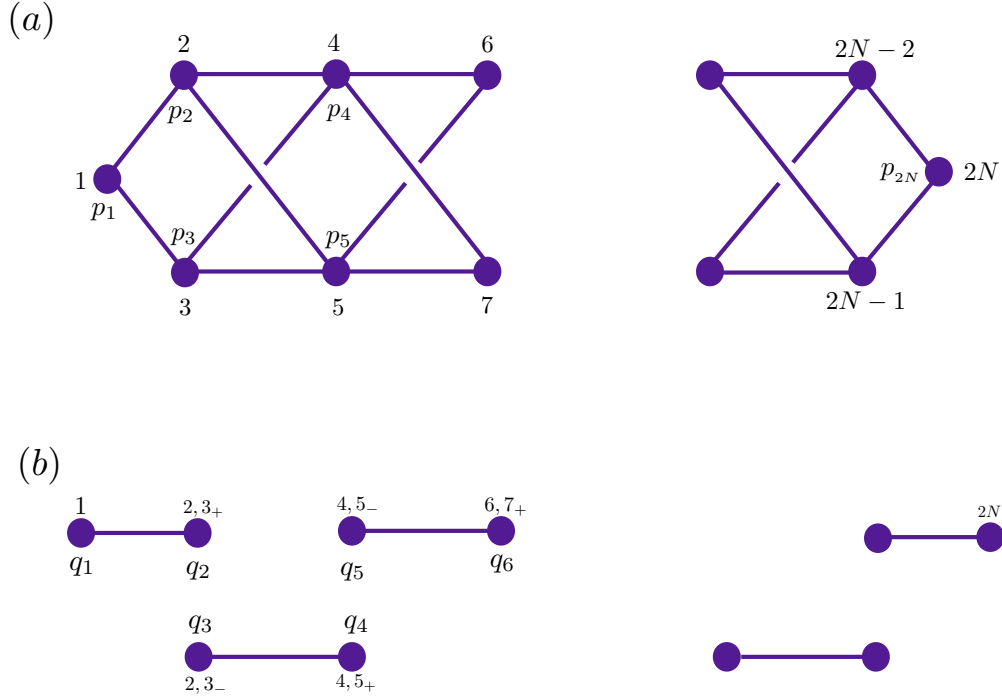


Figure 2: The site probabilities on the actual chain are denoted by p_k , while those on the virtual chains by q_k . The probabilities on the virtual sites are determined from the probabilities on the actual sites above them, i.e. q_2 and q_3 are determined by p_2 and p_3 and so on as in (23) and (24).

where integers n_k are arbitrary. Also from (13) one finds

$$2J_k(\tau_k - \tau_{k+1}) = m_k\pi + \cos^{-1} \sqrt{\frac{q_{2k-1} + q_{2k}}{A_{k-1}^2}}, \quad m_k \in \mathbb{Z}, \quad k = 1, \dots, N, \quad (16)$$

where again, the integers m_k have to be chosen judiciously. We will later argue that it is best to set the integers $m_k = 0$ and $n_k = N$ to keep the couplings J_k bounded. Summing (16) and (15) and setting $k = 1$, we find

$$2J_1\tau_1 = N\pi + \cos^{-1} \sqrt{q_1 + q_2} + \cos^{-1} \sqrt{\frac{q_1}{q_1 + q_2}}. \quad (17)$$

Naturally, this single equation does not yield the values of J_1 and τ_1 independently since after all the time scale of the full dynamics can be tuned by the strength of the first coupling constant. However, from the two equations, all the other times and coupling constants can be determined. Dividing (15) by (16) and rearranging one finds:

$$\frac{\tau_{k+1}}{\tau_k} = \frac{N\pi + \cos^{-1} \sqrt{\frac{q_{2k-1}}{q_{2k-1} + q_{2k}}}}{N\pi + \cos^{-1} \sqrt{\frac{q_{2k-1} + q_{2k}}{A_{k-1}^2}} + \cos^{-1} \sqrt{\frac{q_{2k-1}}{q_{2k-1} + q_{2k}}}}.$$

which after repeating and using (17) yields

$$\tau_{k+1} = \frac{1}{2J_1} \frac{\prod_{i=1}^k [N\pi + \cos^{-1} \sqrt{\frac{q_{2i-1}}{q_{2i-1} + q_{2i}}}]}{\prod_{i=1}^{k-1} [N\pi + \cos^{-1} \sqrt{\frac{q_{2i+1} + q_{2i+2}}{A_i^2}} + \cos^{-1} \sqrt{\frac{q_{2i+1}}{q_{2i+1} + q_{2i+2}}}]}. \quad (18)$$

From (15) we can now determine all the coupling strengths:

$$J_k = J_1 \prod_{i=1}^{k-1} \left[\frac{N\pi + \cos^{-1} \sqrt{\frac{q_{2i+1} + q_{2i+2}}{A_i^2}} + \cos^{-1} \sqrt{\frac{q_{2i+1}}{q_{2i+1} + q_{2i+2}}}}{N\pi + \cos^{-1} \sqrt{\frac{q_{2i-1}}{q_{2i-1} + q_{2i}}}} \right]. \quad (19)$$

We now determine the order of magnitude of couplings J_k . Since $\cos^{-1}(\cdot) \in [0, \pi/2]$ according to Eq. (19) for large N :

$$\frac{J_k}{J_1} \leq \prod_{i=1}^{k-1} \left[\frac{N\pi + \frac{\pi}{2} + \frac{\pi}{2}}{N\pi} \right] = \left(1 + \frac{1}{N}\right)^{k-1} < \left(1 + \frac{1}{N}\right)^N \simeq e, \quad (20)$$

and

$$\frac{J_k}{J_1} \geq \prod_{i=1}^{k-1} \left[\frac{N\pi}{N\pi + \frac{\pi}{2}} \right] = \frac{1}{\left(1 + \frac{1}{2N}\right)^{k-1}} > \frac{1}{\left(1 + \frac{1}{2N}\right)^N} \simeq \frac{1}{\sqrt{e}}. \quad (21)$$

In deriving these bounds, the choice $m_k = 0$, $n_k = \pi$ has played a crucial role and the result is that the order of magnitude for J_k and J_1 are the same. Thus there is no exponential increase in the value of coupling constants or exponential decrease in the time interval between the pulses.

3.1.2 Given probabilities in the spin network

The evolution of the spin network could be obtained from the evolution of the virtual spin chains. By inserting Eq. (11) in Eq. (8) we have:

$$e^{-iHt}|1\rangle = \sum_{k=1}^N [(-i)^{k-1} \sqrt{q_{2k-1}} |2k-2, 2k-1\rangle + (-i)^k \sqrt{q_{2k}} |2k, 2k+1\rangle]$$

Using the definitions of $|i, j_{\pm}\rangle := \frac{1}{\sqrt{2}}(|i\rangle \pm |j\rangle)$ this state is equivalent to the following state on the actual chain

$$e^{-iHt}|1\rangle = \sum_{k=1}^N \frac{(-i)^k}{\sqrt{2}} (\sqrt{q_{2k}} + \sqrt{q_{2k+1}}) |2k\rangle + \sum_{k=0}^{N-1} \frac{(-i)^k}{\sqrt{2}} (\sqrt{q_{2k}} - \sqrt{q_{2k+1}}) |2k+1\rangle. \quad (22)$$

Since we want to generate a state $|\psi_T\rangle = \sum_{n=1}^{2N} \alpha_n |n\rangle$ where $|\alpha_n|^2 = P_n$, this gives

$$P_{2k} = \frac{1}{2} (\sqrt{q_{2k}} + \sqrt{q_{2k+1}})^2, \quad P_{2k+1} = \frac{1}{2} (\sqrt{q_{2k}} - \sqrt{q_{2k+1}})^2 \quad (23)$$

or equivalently:

$$q_{2k} = \frac{P_{2k} + P_{2k+1}}{2} + \sqrt{P_{2k} P_{2k+1}} \quad ; \quad q_{2k+1} = \frac{P_{2k} + P_{2k+1}}{2} - \sqrt{P_{2k} P_{2k+1}} \quad (24)$$

Therefore for any set of given probabilities on the actual chain, one can immediately determine the probabilities on the virtual chain and then from (19) and (18) tune the coupling strengths and the pulse times to generate that give state. A minor simplification arises if we demand that the state has support only on the lower or upper branch of the quasi-one-dimensional chain, i.e. on the chain consisting of even-numbered qubits or odd-numbered qubits. In these cases where we use one of the branches as the main chain and the other branch as the ancilla chain, we are in fact dealing with a one-dimensional chain and in these cases, we have $P_{2k}P_{2k+1} = 0$ and from (24), we have $q_{2k} = q_{2k+1}$.

4 Examples

In this section use the above mechanism to generate some well-known states. (1) W-states with equal probability of having an excited spin in each site and (2) Gaussian-states of different widths.

Remark: In our examples, we use the lower part of the network, the sites with odd index, only as ancillary qubits. That is the amplitude on all these sites are zero and the state is supported only on the above leg of the chain, i.e. on the even-numbered spins. So in both examples, the lower chain is empty and the state is generated on the above chain of even-numbered qubits.

4.1 W-states

For W-states the probabilities in the upper chain are equal and in the lower chain are zero:

$$\forall k \in \{1, 2, \dots, N\} : P_{2k-1} = 0, \quad P_{2k} = \frac{1}{N}.$$

Therefore, we can find the probabilities in the virtual chains:

$$q_1 = 0, \quad \forall k \in \{1, 2, \dots, N-1\} : q_{2k} = q_{2k+1} = \frac{1}{2N}, \quad q_{2N} = \frac{1}{N}.$$

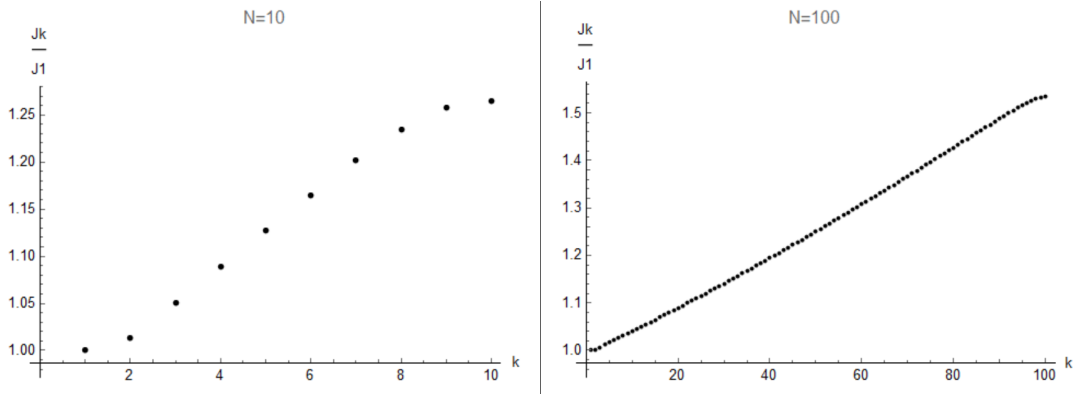


Figure 3: The coupling strengths for generating the W-states on chains of length $N=10$ and $N=100$.

The coupling strengths are found from (19) and the times from (18). The results are shown in figures (3) and (4) for chains of length 10 and 100.

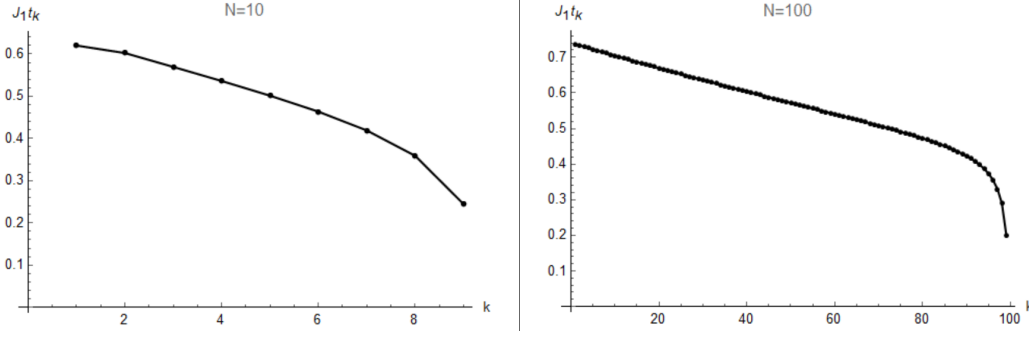


Figure 4: The time sequence of Z_k pulses for generating W states on chains of length $N=10$ and $N=100$ sites. t_k is the time lapse between the k -th pulse and the $k+1$ -th pulse.

4.2 Gaussian-states

To generate a Gaussian state of a given width on the upper chain, we fix

$$\forall k \in \{1, 2, \dots, N\} : P_{2k-1} = 0, \quad P_{2k} = \frac{e^{-\frac{(k - \frac{N+1}{2})^2}{2\sigma^2}}}{\sqrt{2\pi\sigma^2}}. \quad (25)$$

From which we find

$$q_1 = 0, \quad \forall k \in \{1, 2, \dots, N-1\} : q_{2k} = q_{2k+1} = \frac{e^{-\frac{(k - \frac{N+1}{2})^2}{2\sigma^2}}}{2\sqrt{2\pi\sigma^2}}, \quad q_{2N} = \frac{e^{-\frac{(\frac{N-1}{2})^2}{2\sigma^2}}}{\sqrt{2\pi\sigma^2}}.$$

The coupling strengths and time sequences of pulses are shown in Fig.5 and 6 for $N=10$ and $N=100$ and for different values of σ .

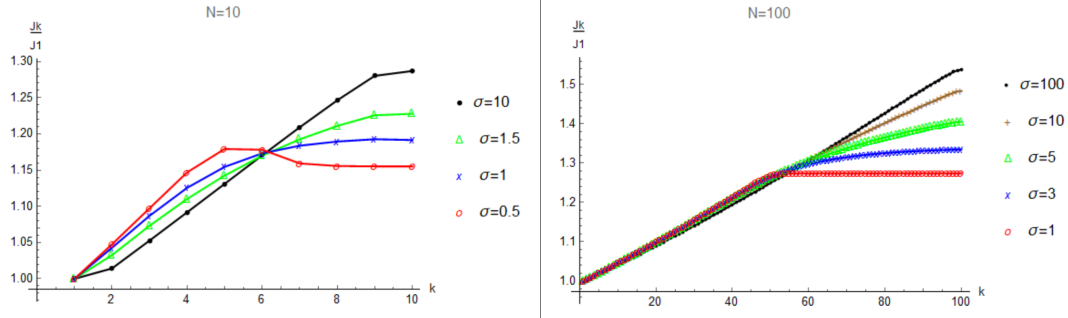


Figure 5: The coupling strengths for generating the Gaussian-states for $n=10$ and $n=100$.

By comparing Fig.3 and Fig.5, we can see that the coupling strengths for generating W-states are very similar to the coupling strengths for generating Gaussian-states with a large standard deviation σ . It meets our expectation since Gaussian-states lead to W-states in the limit of a large standard deviation. By choosing the integers $m_k = 0$ and $n_k = N$ in equations (15) and (16), we have kept all the coupling constants finite and within the bounds provided in (20 and 21).

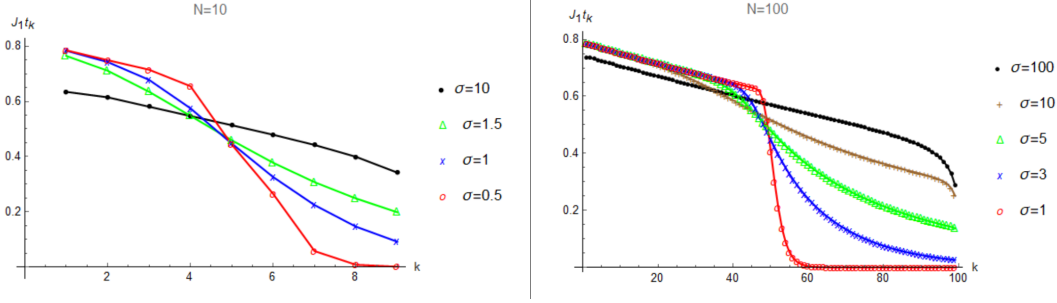


Figure 6: The time sequence of Z_k pulses for generating Gaussian states with various widths. t_k is the time lapse between the k -th pulse and the $k+1$ -th pulse. It is seen that after a while all the pulse can be applied simultaneously, specially for wave packets of small width. The reason is that after the localized packet has been generated, the excitation is effectively confined in the virtual chains in the middle of the chain. Hereafter, all the pulses on the empty chains on the right have no effect on the state.

5 The sensitivity of the scheme against the timing of pulses

As equation (18) shows, it seems that the exact states which are produced depend very much on the precise timing of the applied pulses. It is thus natural to ask how sensitive this scheme is with respect to this timing? What happens if the pulses are not applied exactly at the times demanded by Eq. (18). We have done a detailed analytical treatment of this problem. However, reporting the details is not so illuminating and instead, we report the basic idea and the final numerical results. To simplify the analysis, let us assume that the times of free dynamics in all virtual 2-chains are dilated or contracted by an amount ϵ . This means that there is an accumulative error in the time of all pulses, that is, the first pulse is applied with an offset error of ϵ , the second pulse with an offset error of 2ϵ , the third pulse with an offset error of 3ϵ , and so on. Our intuitive reasoning that this type of error, instead of a random error taken from a distribution, is the worst error that may happen is the following. The whole purpose of the pulses is to transfer an excitation from a virtual chain to the next virtual chain on the right time and if this transfer is delayed in each virtual chain, there comes a time where no excitation is in the middle of the chain to be transferred to the right end of the chain. In this case, the excitation will be trapped in some part of the left-hand side of the chain and goes back and forth in the virtual chains by the natural dynamics of these short chains. In this way, consecutive delays in these transfers hinders the desirable distribution of the excitation on the whole chain. We have calculated the fidelity of the resulting state with the ideal state generated by exactly applied pulses. The results are shown in figure (7) for the W-state and in figure (8) for the Gaussian state. The interesting point is the $\frac{1}{N}$ scaling of the required precision ϵ with the length of the chain for both types of states.

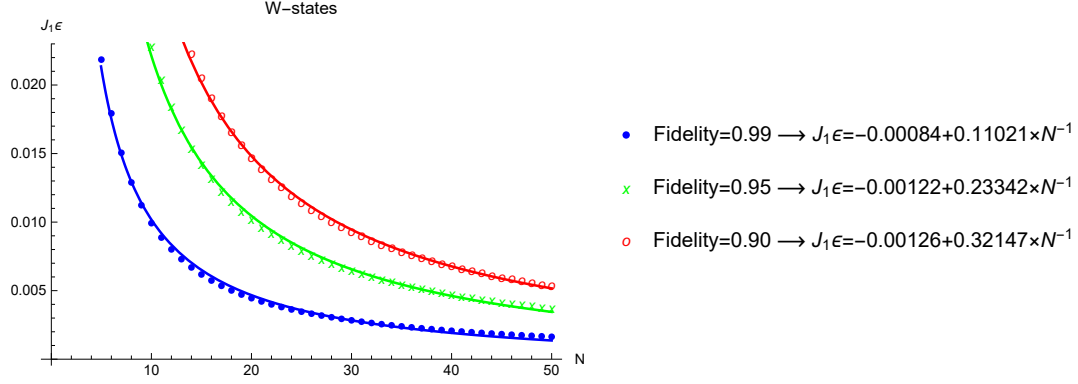


Figure 7: (Color online) The fidelity of the generated W-state with the ideal W-state for chains of different lengths. The blue line separates the plane into regions of fidelity higher than 0.99 (below the curve) and lower than 0.99 (above the curve). This shows, for example that for chains of length $N = 10$ and 20 there is a tolerance of approximately $J_1 \epsilon$ equal to 0.010 and 0.005 respectively. For lower fidelity, the green and red curves, this tolerance naturally becomes higher. The curves from bottom to top are, blue, green and red. Note the nice scaling of the tolerance with the length of the chain written on the right-hand side of the plot. Note that $J_1 \epsilon$ is the dimensionless quantity which should be tuned in order to attain a fidelity.

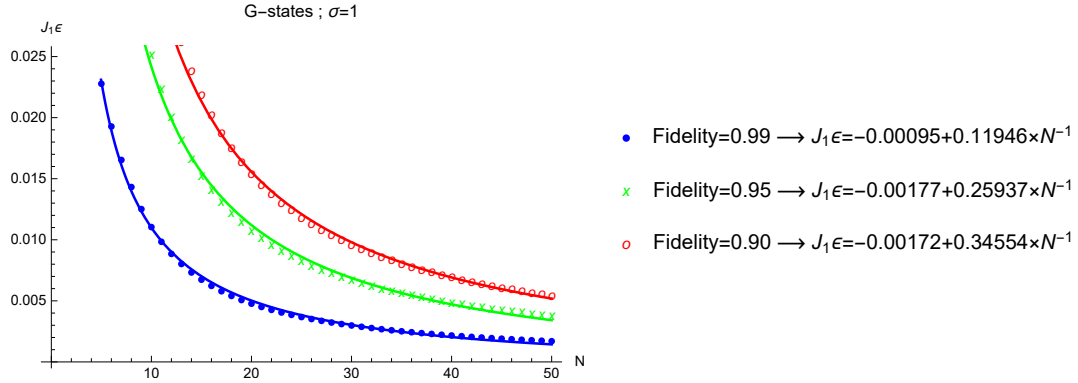


Figure 8: (Color online) Exactly the same description of the figure (7) applies for this plot with the replacement of W-state with Gaussian states with $\sigma = 1$. Only the curves for $\sigma = 1$ are shown, the curves for other values of σ are similar in shape with slightly different numerical factors.

6 Conclusion

In this work and inspired by a technique first introduced in [16] and further developed in [17], we could exactly determine the coupling constants of a quasi-one-dimensional chain which is capable to generate any arbitrary single excitation state. Instead of local magnetic fields B_k which should be tuned along with the coupling constants J_k in the work of [19], we had to use local pulses which have to be applied at definite times. By decomposing the chain into non-interacting virtual chains of length two whose dynamics is a simple rotation, we could exactly generate any single excitation state. Examples of W – states and Gaussian states were studied the results of which are shown in figures 3 and 5. Although the chain seems to be quasi-dimensional and of a particular geometry, we can confine the state entirely on the upper chain and use the lower chain as an ancillary chain which is empty at the end of the process.

7 Acknowledgements

We would like to thank members of the QIS group in Sharif or their valuable comments when this work was presented by one of the authors. This research was partially supported by a grant no. 96011347 from the Iran National Science Foundation. The work of V. K. was also partially supported by a grant from the research grant system of Sharif University of Technology.

References

- [1] S. Bose, Phys. Rev. Lett. **91** 207901 (2003).
- [2] S. Bose, Contemp. Phys. **48**, 13 (2007).
- [3] M. Christandl, N. Datta, A. Ekert, and A. J. Landahl, Phys. Rev. Lett. **92**, 187902 (2004). M. Christandl, N. Datta, T. C. Dorlas, A. Ekert, A. Kay, and A. J. Landahl, Phys. Rev. A **71**, 032312 (2005).
- [4] D. Burgarth and S. Bose, New Journal of Physics **7**, **135** (2005), ISSN 1367-2630.
- [5] A. Kay, Physical Rev. A **73**, 032306 (2006).
- [6] C. Di Franco, M. Paternostro, and M. S. Kim, Phys. Rev. Lett. **101**, 230502 (2008).
- [7] C. Di Franco, M. Paternostro, and M. S. Kim, Phys. Rev. A **81**, 022319 (2010).
- [8] A. Bayat and S. Bose, Phys. Rev. A **81**, 012304 (2010).
- [9] A. Kay, Int. J. Quantum Inform. **8**, 641 (2010).
- [10] P. Jurcevic, et al, Nature **511**, 202 (2014).
- [11] J. I. Latorre, E. Rico, G. Vidal, Quant.Inf.Comput. **4** (2004) 48-92.
- [12] L. Banchi, T. J. G. Apollaro, A. Cuccoli, R. Vaia, and P. Verrucchi, Phys. Rev. A **82**, 052321 (2010).
- [13] R. Raussendorf, D. E. Browne, H. J. Briegel, Phys. Rev. A **68**, 022312 (2003).
- [14] S. C. Benjamin and S. Bose, Phys. Rev. Lett. **90**, 247901 (2003).
- [15] A. Kay, and M. Ericsson, New J. Phys. **7**, 143 (2005).

- [16] P. J. Pemberton-Ross and A. Kay, Phys. Rev. Lett. **106**, 020503 (2011).
- [17] V. Karimipour, M. Sarmadi Rad and M. Asoudeh, Phys. Rev. A **85**, 010302 (2012).
- [18] M Asoudeh, V Karimipour, Quantum information processing 13 (3), 601-614.
- [19] A. Kay, New. J. Phys. **19**, 043019 (2017).
- [20] M. Paternostro, G. M. Palma, M. S. Kim, G. Falci, Phys. Rev. A 71, 042311 (2005), A. Romito, R. Fazio and C. Brudo, Phys. Rev. B 71, 100501(R) (2005), A. Lyakhov and C. Bruder, New J. Phys. 7, 181 (2005).